2025 International Conference on Space Robotics (iSpaRo)
December 1-4, 2025, Sendai, Japan

Design and Performance Evaluation of a Scalable Rectenna for Microwave Wireless Charging of Modular Lunar Robots

A. Sejal Jain[1], Shreya Santra[1], Hiroyasu Sato[2],Qiang Chen[2] and Kazuya Yoshida[1]

2025 International Conference on Space Robotics (iSpaRo) | 979-8-3315-6020-1/25/$31.00 ©2025 IEEE | DOI: 10.1109/iSpaRo66239.2025.11437049

***Abstract*— This study presents the design, development, and evaluation of a microwave-based wireless power transmission (MWPT) system to enable efficient, cable-free power delivery to modular robotic systems on the lunar surface. Focusing on MoonBot—an autonomous, reconfigurable robot developed under Japan's Moonshot R&D program, the research proposes a scalable rectenna system to receive microwave power and wirelessly charge MoonBots deployed for tasks such as lunar exploration and outpost construction. A $2.45\,\mathrm{GHz}$ rectenna prototype was developed using a hexagonal patch antenna and a Schottky-diode-based rectifier with 81.7% and 85% RF–DC conversion efficiency at $1\,\mathrm{W}$ and $1.3\,\mathrm{W}$ input powers respectively. Scaled multi-element configurations were tested to evaluate end-to-end system performance. Far-field simulations were extended to distances up to $1000\,\mathrm{m}$, revealing that a 100-element rectenna can deliver $100\,\mathrm{W}$ of rectified DC power with a transmitted power of $15.17\,\mathrm{MW}$. Furthermore, compact honeycomb layout arrangement of rectenna elements was proposed to enhance power capture and reduce required transmission power. Based on these results, estimated charging times for different MoonBot configurations were calculated. This research demonstrates a scalable and functional MWPT receiver prototype for the potential development of wireless power infrastructure for modular lunar robots.**

I. Introduction

Robotic systems have been indispensable in extending human reach to hostile extraterrestrial environments. These autonomous platforms have enabled scientific discovery, experimentation and exploration in inaccessible regions. From the early Lunokhod and Apollo Lunar Vehicles to modern rovers like Pragyaan, Yutu-2, VIPER and Perseverance, these platforms have significantly advanced planetary surface exploration [1]. However, as space programs now shift their focus to long-term habitation and infrastructure development, the role of robotic systems must evolve accordingly. In addition to exploration, next generation robotic systems are expected to autonomously build habitats, manage infrastructure, and support continuous surface operations.

To address these future needs, Japan's Moonshot Research and Development Program (Goal 3) sets an ambitious vision to develop Self Evolving AI (Artificial Intelligence) Robot System for Lunar Exploration and Human Outpost Construction by 2050. One of the key developments under this initiative is its ground prototype, MoonBot—a modular, reconfigurable robotic system engineered by the Space Robotics Laboratory (SRL) at Tohoku University [2]. MoonBot comprises a set of functional modules, such as 7-degree-of-freedom limbs, wheels, and manipulators that can autonomously assemble, adapt, and reconfigure for diverse tasks such as building lunar infrastructure, deploying vertical solar panels and transporting essential units.

*This work was supported by JST Moonshot R&D Program, Grant Number JPMJMS223B.

[1] A. Sejal Jain, S. Santra and K. Yoshida are with the Department of Aerospace Engineering, [2] Hiroyasu Sato and Qiang Chen are with Department of Communications Engineering, Graduate School of Engineering, Tohoku University, Sendai 980–8579, Japan.
The corresponding author is A. Sejal Jain
(E-mail: anil.sejal.jain.r1@dc.tohoku.ac.jp)

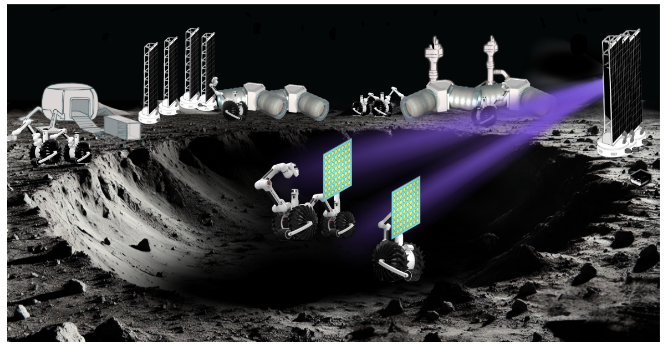

Fig. 1. Conceptual illustration of microwave-based wireless power transfer to MoonBot-Dragon and MoonBot-Minimal configurations. ©SRL

However, MoonBot's modularity and functional versatility requires a power supply system that is adaptable, reliable, and scalable. Traditional power systems such as solar panels, radioisotope thermoelectric generators (RTGs), and wired power grids fall short under lunar conditions. Solar power is limited by prolonged darkness and shadowed terrain [3]; RTGs, while continuous, are costly, heavy, and pose safety concerns [4]; and constraints associated with wired grid systems makes it unfeasible to deploy and maintain across the lunar surface [5]. Solar reflector-based systems rely on continuous sunlight making them impractical beyond a few kilometres. Adding secondary or tertiary reflectors increases structural complexity and maintenance requirements [6]. Laser systems offer long-distance transmission but suffer from low conversion efficiency (20–40%), high heat losses, safety concerns and precise alignment needs [7].

This research proposes microwave-based wireless power transmission (MWPT) as a viable solution for delivering power over long distances without physical connectors, illustrated in Fig. 1. This study presents the design, fabrication, and performance evaluation of a rectenna prototype—a combined antenna and rectifying circuit optimized for $2.45\,\mathrm{GHz}$ operation. Based on these results, scaled-up simulations were conducted to evaluate rectenna's performance in charging different MoonBot configurations. The prototype was adapted for watt-level power delivery, and end-to-end power transfer was estimated over distances from a few metres to kilometre-scale.

II. Related Works

Microwave-based wireless power transfer offers a cable-free alternative to conventional power systems. Operating within ISM bands such as 2.45, 5.8, 24, and 35 GHz, MWPT systems convert DC power into RF signals, transmit them via high-gain antennas, and recover usable DC power using rectenna [8].

The first practical demonstration of MWPT was in 1964 by William C. Brown, who powered a helicopter at 2.45 GHz. A landmark 1975 experiment at NASA's JPL Goldstone Facility transmitted 450 kW over 1.6 km, achieving 82.5% rectification efficiency and 30 kW DC output [9]. In the 1990s, Canada's SHARP project powered a fuel-free aircraft at 150 m altitude using a 10 kW, 2.45 GHz microwave beam, while Japan's MILAX project powered a hovering aircraft using a 2.411 GHz phased array [8].

The 21st century has witnessed a broad expansion of MWPT use cases. At Kyoto University, an agricultural rover was powered by an 800 W, 2.45 GHz source, receiving 41 W over a few meters [10]. A Mars aircraft prototype achieved flight at 3 m using 900 W of transmitted power and 15 rectennas [11]. Ozawa and Tanaka demonstrated wireless flight at 58 m, delivering 166 W using a 10 kW, 5.8 GHz source [12]. Volvo Technologies Japan developed a top-to-roof EV charging system operating at 2.45 GHz, achieving $3.2\,\mathrm{kW/m^2}$ power density at 4 m [13]. Space-based solar power (SBSP) concepts and prototype demonstrations in the United States, Japan, China, European Union, and United Kingdom have investigated the feasibility of transmitting power over hundreds to thousands of kilometres from orbiting solar platforms to Earth-based rectenna arrays [8].

These studies and demonstrations show that MWPT uses moderately focused beams, requiring larger rectennas. Microwave receiver systems have demonstrated RF-DC rectification efficiency reaching up to 90%, especially at lower frequencies [14]. Advances in beam steering and phased array have simplified beam alignment, allowing MWPT systems to track and power moving targets easily compared to other wireless power technologies.

The main contribution of this work is as follows: Design and development of a scalable rectenna prototype capable of delivering up to 1 W of DC output per element is presented in section III. The rectenna is scaled to multi-element configurations and evaluated through electromagnetic–circuit co-simulations for end-to-end power transfer, with results validated experimentally in section IV. To meet the power demands of MoonBot configurations, section V presents simulations of further scaled versions of the prototype using asymptotic solver, optimized for electrically large distances ranging from 5 m to 1000 m. A compact honeycomb rectenna is also proposed to improve power capture efficiency and reduce transmission power requirements. Section VI presents the estimation of battery charging times for the MoonBot configurations at various transmission distances.

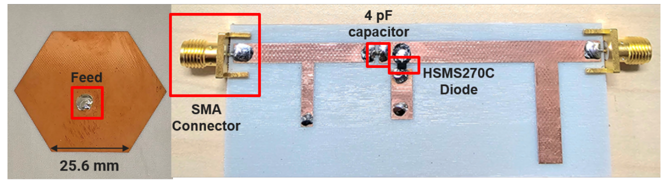

Fig. 2. Fabricated hexagonal coax-fed patch antenna and rectifier circuit

III. Methodology

A. Rectenna design

A rectenna consists of an antenna and a rectifying circuit. Both components are individually simulated at 2.45 GHz, followed by fabrication and experimental validation. The goal is to evaluate received power, RF-DC conversion efficiency, impedance matching, and output voltage characteristics under low load conditions for battery charging. The receiver antenna is designed as a coaxial-fed hexagonal patch antenna in CST-Microwave Studio [15]. The hexagonal patch offers a compact footprint with circular patch-like current distribution, higher gain, broader bandwidth, and improved impedance matching over rectangular patches. It was designed on a NPC H220A substrate ($\varepsilon_r = 2.17$, $H = 1.6\,\mathrm{mm}$). The radius a of an equivalent circular patch at 2.45 GHz was calculated and then converted to the side length l of a hexagon using area equivalence:

$$a = \frac{\frac{8.791\times10^9}{f_r\sqrt{\varepsilon_r}}}{\left\{1+\frac{2h}{\pi\varepsilon_r F}\left[\ln\left(\frac{\pi F}{2h}\right)+1.7726\right]\right\}^{1/2}}; \pi a^2 = l^2\cdot\frac{3\sqrt{3}}{2} \tag{1}$$

Based on these calculations, the side length of the hexagonal patch was $l = 25.6\,\mathrm{mm}$. The ground plane measured 80 mm × 80 mm and the distance from the centre of the patch to the feed point is 5.89 mm.

The RF–DC rectifier circuit is designed using the HSMS-270C Schottky diode (Avago Technologies), selected for its sufficient breakdown voltage (25 V) and suitable spice parameters to produce 1 W rectified output. Unlike conventional single-shunt rectifier topologies that use a low-pass filter, the design replaces it with a band-stop filter to suppress harmonics, particularly the second harmonic ($2f_0$), where $f_0 = 2.45\,\mathrm{GHz}$. It also exhibits inductive impedance that offsets diode capacitance, improving impedance matching.

The circuit is modelled in Keysight ADS [16] on the same substrate as the antenna. The rectifier's input impedance is matched with the antenna using lumped elements realized as microstrip lines. A 4 pF DC block capacitor isolates the RF and DC parts of the circuit. A short-circuited $\lambda/8$ line in series with the diode, functions as a band-stop filter, while a series $\lambda/4$ transmission line and a parallel open-circuited line, combines as DC bypass filter. The circuit terminates with a $100\,\Omega$ load, suitable for interfacing with a DC–DC buck-boost converter for battery charging applications. The fabricated hexagonal patch antenna and rectifier circuit is displayed in Fig. 2.

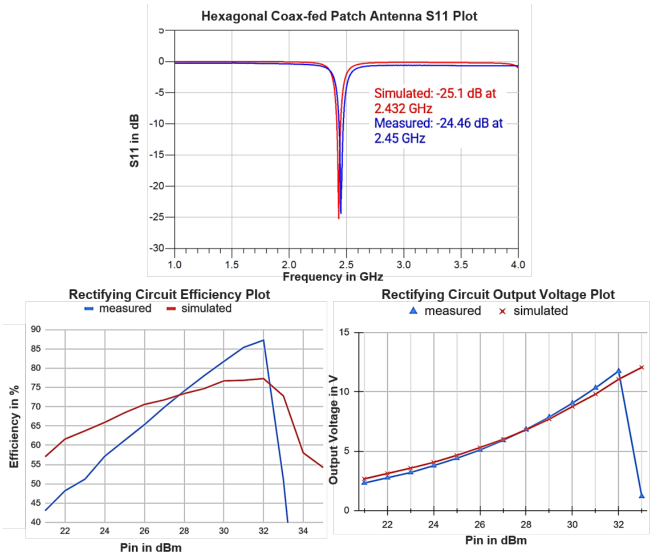

Fig. 3. Simulation versus experimental measurement plots for both hexagonal patch antenna and rectifier circuit

B. Rectenna Simulation and Fabrication results

After simulation and optimisation trials, the designed antenna was fabricated and tested using a Vector Network Analyzer (VNA) in an anechoic chamber. The measured return loss, S_{11} was $-24.46\,\text{dB}$ at $2.45\,\text{GHz}$, with an impedance of $57.06 - j2.05\ \Omega$, close $50\,\Omega$ reference impedance. The gain was measured to be $7.9\,\text{dBi}$ using a reference dipole antenna(theoretical gain of $2.15\,\text{dBi}$) placed $2\,\text{m}$ away. The simulation versus experiment S_{11} plot is depicted in Fig. 3.

To enhance power capture over longer transmission distances, two multi-element configurations were developed: a 4-element (2×2) grid and a 7-element hexagon layout, both with 0.5λ spacing. Simulated gains were $11.6\,\text{dBi}$ and $13.8\,\text{dBi}$, with beamwidths of $47.8°$ and $38.4°$, respectively. When fabricated and measured, the S_{11} values were in the range of $-13\,\text{dB}$ to $-16\,\text{dB}$ and impedance of $\approx 35 + j7\ \Omega$ for each element. A slight degradation in S_{11} is observed due to mutual coupling between antennas, yet remains below the $-10\,\text{dB}$ threshold.

The rectifier circuit's non-linear behaviour was analysed using the Harmonic Balance simulator which computes its steady-state response under single-frequency excitation. Following the simulation, a layout was analysed using Momentum EM simulator to model parasitic, coupling, and physical layer effects for real-world circuit behaviour. The RF–DC conversion efficiency, $\eta_{\text{RF-DC}}$ [17], is calculated using:

$$\eta_{\text{RF-DC}} = \frac{V_{\text{load}}^2}{P_{\text{in}} \cdot R_{\text{load}}} \times 100 \tag{2}$$

where V_{load} is the DC output voltage, P_{in} is the input RF power, and R_{load} is the load resistance.

The simulation versus measurement plots for RF-DC efficiency and output voltage are shown in Fig. 3. When fabricated and tested for $1\,\text{W}$ input at $2.45\,\text{GHz}$, the rectifier achieved a RF–DC efficiency of 81.72%, with a DC output of $9.04\,\text{V}$. At $1.3\,\text{W}$ input power, the RF-DC efficiency is about 85%, delivering $10.3\,\text{V}$. The difference between simulation and experimental results could be due to diode model variations or better impedance matching via the direct connection to power amplifier.

IV. End-to end MWPT measurement for the proposed rectenna

After individually testing the rectenna components, it is essential to integrate them in a far-field MWPT setup. At far-field distances, the emitted microwaves from a transmitting antenna(Tx) behave like planar waves with uniform electric and magnetic field distributions, making energy estimation easier at a distant rectenna(Rx). However, as the wavefront expands, propagation loss occurs, reducing power density with distance. This loss is quantified by the *Friis transmission equation* [17]:

$$P_{\text{Rx}} = P_{\text{Tx}} G_{\text{Tx}} G_{\text{Rx}} \left(\frac{\lambda}{4\pi D_r} \right)^2 \tag{3}$$

where P_{Rx} is the received RF power, P_{Tx} is the transmitted RF power, G_{Tx}, G_{Rx} are the antenna gains, λ is the wavelength at resonant frequency and D_r = distance between transmitter and rectenna. This equation shows that received power decreases with the square of the distance. To ensure far-field conditions, the minimum required distance is:

$$D_r \geq \frac{2R^2}{\lambda} \tag{4}$$

where R is largest dimension of either of the two antennas.

To evaluate far-field MWPT end-to-end efficiency, a co-simulation using CST Transient solver and ADS was performed. CST modelled behaviour and propagation losses between the transmitting antenna and rectenna at various distances. These data were input into ADS to analyse the rectenna and estimate the rectified DC power for a given transmitted RF power. The simulations were compared with the experiments conducted in an anechoic chamber.

A. Transmitter and 7-element rectenna separated by $2\,\text{m}$

In this experiment (Fig. 4), a horn antenna (SWH-22, ARA Technologies Inc.) was used as the transmitter, and a 7-element rectenna as the receiver, with each element connected to its own rectifying circuit. The system was powered by an RF generator (TZ3ZZDD, Tokyo Keiki Ltd.) operating from 2.4-2.5 GHz, sweeping input power from $10\,\text{W}$ to $131\,\text{W}$. The load resistance was set to $14.3\,\Omega$, corresponding to the parallel combination of seven rectifiers. At an input power of $131\,\text{W}$, the measured DC output voltage was $5.49\,\text{V}$, yielding an output power of $2.11\,\text{W}$. Fig. 4(b) compares the rectified output power obtained from Friis estimation, simulation, and experimental measurement.

The lower measured output power could be due to mutual coupling between receiver elements, impedance mismatch (rectifier: $57.06 - j2.05\ \Omega$ vs. antenna: $35 + j7\ \Omega$), slight beam misalignment, and inconsistent load values from the variable resistor affecting the accuracy.

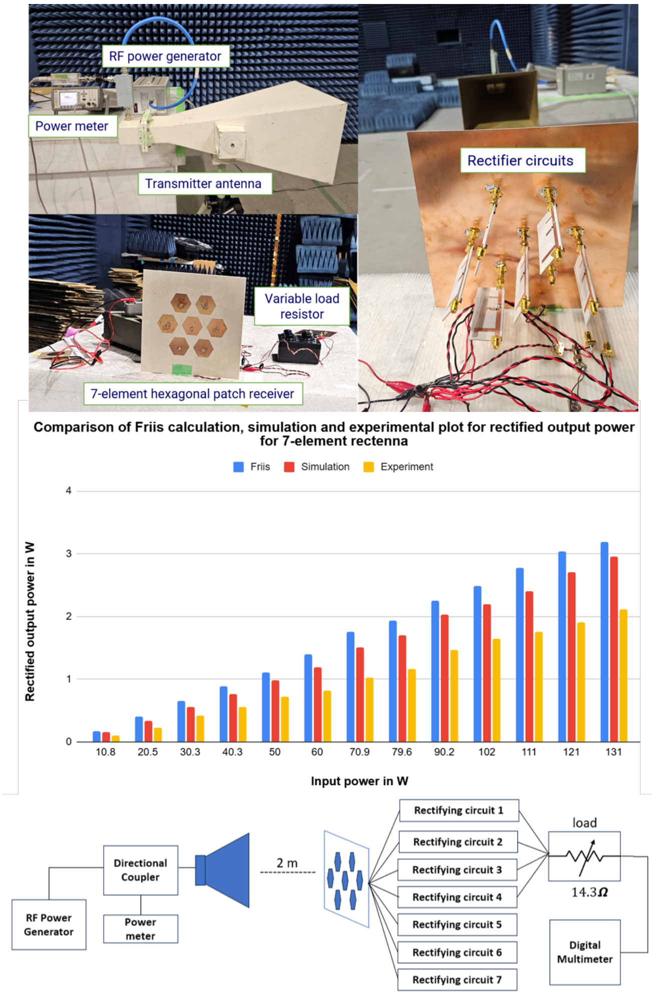

Fig. 4. Experiment setup and rectified output power comparison for end-to-end MWPT at 2 m between a horn transmitter and 7-element hexagonal rectenna in an anechoic chamber.

V. Scaled-up MWPT systems for MoonBot

Each functionally independent module of MoonBot is equipped with its own power supply, a 11.1 V battery for onboard computer and sensors, and a 22.2 V battery for actuators. To evaluate the end-to-end microwave power transferred to the robots, a baseline rectified output of 100 watts was selected. An array of 100 rectenna elements was optimal for achieving this target. Simulations were conducted for power reception at distances of 5 to 1000 meters from a fixed transmitter.

A. Simulation Methodology

For electrically large distances (hundreds to thousands of meters), CST Asymptotic solver is used, as transient solver becomes impractical due to high computational requirements. The solver simulates beam propagation and displays field distribution and alignment at the rectenna aperture. Power density is calculated and combined with known RF-DC efficiency of the rectifier circuit to estimate DC output. For simplicity, identical antennas were used for both the transmitter and receiver with default CST excitation (unit amplitude, zero phase). No beam-forming or phased-array techniques were applied. Side lobes radiating ≈5% of power outside the main lobe were also neglected.

1) Transmitter and rectenna-equipped MoonBot separated by 5 m*:* A rectenna-equipped MoonBot minimal is positioned 5 m from the transmitter antenna (Fig. 5). To meet far-field criteria at operating frequency, the designed rectenna comprises of 64 elements in an 8×8 grid, measuring $0.525\,\mathrm{m} \times 0.525\,\mathrm{m}$. Simulations indicated a gain of 23.2 dBi, with the first side lobes corresponding to 4.6% (−13.4 dB) of the main lobe power.

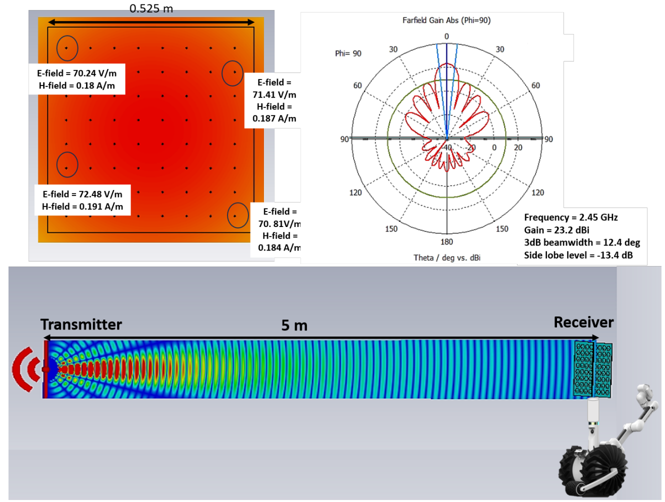

Fig. 5. 64 element rectenna far-field properties, E-field and H-field distributions at rectenna surface and along transmission axis for 5 m distance.

In asymptotic simulations antennas are excited with 0.5 W each, resulting in 27.8 W total power after loss compensation. The simulated time-average E-field (E_{avg}) and H-field (H_{avg}) distributions are nearly uniform across the rectenna surface, with slightly lower values near the corners.

The average power density is calculated using:

$$S = E_{\mathrm{avg}} \times H_{\mathrm{avg}} \tag{5}$$

$$= 76.279 \times 0.2024 = 15.44\,\mathrm{W\,m^{-2}}.$$

Given the rectenna area as $0.276\,\mathrm{m}^2$, power received at the rectenna surface is 4.26 W. With an RF-DC efficiency of 76.5%, each element requires 1.3 W input to deliver 1 W rectified DC power. Thus, to receive 83.2 W at the rectenna surface and obtain 64 W of maximum rectified DC output, the transmitter power is scaled linearly as the field distributions remain unchanged without physical modifications to the transmitter or receiver. The required transmitted power is

$$P_{\mathrm{Tx}} = \frac{83.2}{4.26} \times 27.8 \approx 543\,\mathrm{W}$$

The Friis equation estimates received power at 89.3 W, higher than simulations since it excludes losses from side lobes, mutual coupling, and material absorption.

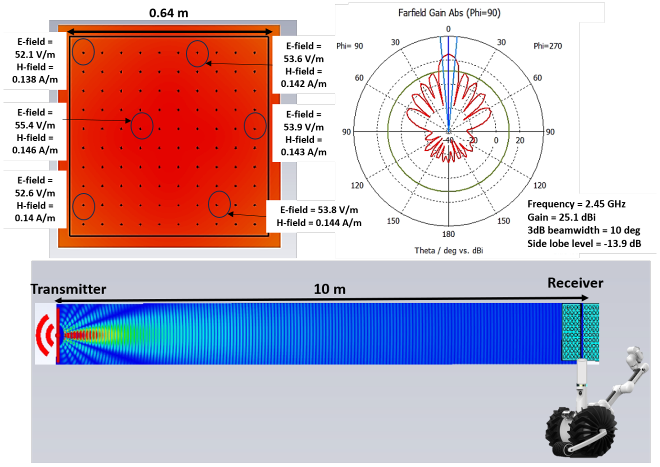

Fig. 6. 100 element rectenna far-field properties, E-field and H-field distributions at rectenna surface and along transmission axis for 10 m distance.

2) Transmitter and rectenna-equipped MoonBot separated by 10 m*:* In this scenario (Fig. 6), the distance between transmitter and rectenna-equipped MoonBot minimal is increased to 10 m. The rectenna is expanded to a 10×10 configuration with dimensions $0.64\,\mathrm{m} \times 0.64\,\mathrm{m}$, satisfying far-field conditions. This configuration, with a measured gain of 25.1 dBi, is adopted as the standard rectenna design for all subsequent distance analyses.

With a line-of-sight setup, the transmitted power to the rectenna is 38.51 W. Simulations show similar E-field and H-field distributions as in the previous case, with an average power density of $8.2\,\mathrm{W\,m^{-2}}$, calculated using equation (5). Given the rectenna area of $0.41\,\mathrm{m^2}$, the resulting power received at the rectenna is 3.36 W.

To receive a target power of 130 W (1.3 W per element), the required transmission power is 1.5 kW. With RF-DC efficiency of 76.5%, the corresponding DC output from the rectenna is approximately 100 W. At the same input level, the Friis equation predicts 143.7 W of power received at the rectenna surface.

Table I summarizes the simulation and Friis-calculated results for achieving 100 W of rectified power at each distance. It highlights the sharp rise in input power required at distances such as 500 m and 1000 m due to the inverse square dependence of the power received at rectenna on distance, obtained from the Friis equation.

B. Modified rectenna to improve MWPT efficiency for the MoonBots

To improve end-to-end efficiency for such long distances, one strategy is to increase the number of antenna elements by using a compact hexagonal honeycomb layout with minimal changes in physical size. This design enables denser packing while maintaining the same inter-element spacing, enhancing both gain and effective aperture area at the rectenna. As a result, more elements can simultaneously capture incoming power without significantly enlarging the rectenna footprint.

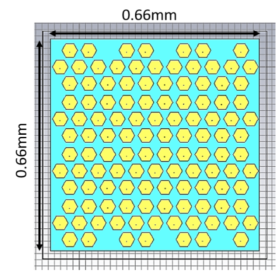

Fig. 7. Compact 118-element hexagonal patch array with central gaps filled to maximize aperture area

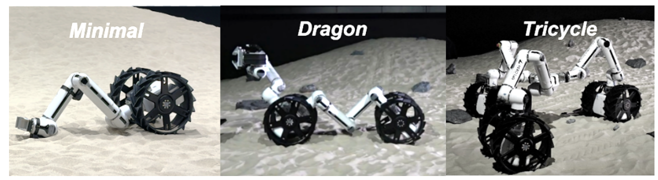

Fig. 8. Various MoonBot configurations [2]

For example, by slightly extending the 100-element rectenna from 0.64 m to 0.66 m (a mere 20 mm extension) on each side, a 118-element honeycomb rectenna configuration can be realized, as shown in Fig 7. Simulations indicated a gain of 26 dBi for the rectenna. With uniform field distribution observed, achieving a total rectified DC output of 118 W at a distance of 1000 m would require approximately 154 W of incident RF power on the rectenna surface. Using the same calculations as in section V-A, the required transmission power is 11.4 MW. This is nearly 4 MW less input power, while yielding higher rectified DC output than the 100-element rectenna.

VI. Charging time Estimation for MoonBot

Due to its modularity, each MoonBot configuration, exhibits distinct power consumption characteristics, determined by the number and type of active functional units. The energy capacities range from 380 Wh for minimal to 1272 Wh for tricycle configurations shown in Fig. 8. The rectified DC power obtained in section V is then fed into a buck-boost converter and a battery management system (BMS) in the MoonBot to safely and efficiently charge its batteries. In practical conditions, their combined efficiency is expected to be 90–95%. The battery charging time is calculated as:

$$\text{Charging Time} = \frac{\text{Battery Capacity}}{\text{Rectified DC power}} \times \eta_{\text{DC-DC/BMS}} \quad (6)$$

Table II summarizes the estimated charging times for each MoonBot configuration at various transmission distances, based on transmitted power and rectified DC output.

VII. Conclusions

A foundational approach for microwave-based wireless power reception system for lunar robots like MoonBot has been presented. A rectenna prototype, featuring hexagonal coaxial-fed patch antenna and a rectifier circuit with over 81% RF-DC conversion efficiency for input between

TABLE I

SIMULATION AND THEORETICAL RESULTS FOR RECTIFIED OUTPUT OF 100 W AT VARIOUS TRANSMITTER-RECTENNA DISTANCES

Transmission Distance (m)	**CST Simulation Results**						**Friis Calculation Results**	
	Input power (W)	**Received power Density (W/m^2)**	**Received Power (W)**	**Required received power (W)**	**Required transmission power (W)**	**Rectified Power (W)**	**Required received Power (W)**	**Rectified power (W)**
5	27.8	15.44	4.26	83.2	543	64	89.3	68.3
10	38.51	8.2	3.36	130	1.5 x 10^3	100	143.7	110
100	38.51	82.1 x 10^{-3}	33.62 x 10^{-3}	130	0.148 x 10^6	100	142.62	109
500	38.51	3.3 x 10^{-3}	1.35 x 10^{-3}	130	3.7 x 10^6	100	141.6	108.3
1000	38.51	0.81 x 10^{-3}	0.33 x 10^{-3}	130	15.17 x 10^6	100	145.2	111

TABLE II

CHARGING TIME FOR VARIOUS MOONBOT CONFIGURATIONS

Distance (m)	**Transmitted Power (W)**	**Rectified Power (W)**	**Charging Times (in hours) for MoonBots**		
			Minimal (380 Wh)	**Dragon (760 Wh)**	**Tricycle (1272 Wh)**
5	543	64	6.2 – 6.5	12.4 – 13	20.8 – 21.5
10	1.5 x 10^3	100	4 – 4.2	8 – 8.4	13.4 – 14
100	0.148 x 10^6	100			
500	3.7 x 10^6	100			
1000	15.17 x 10^6	100			
1000	11.4 x 10^6	118	3.4 – 3.6	6.8 – 7.2	11.4 – 12

with 1 W and 1.5 W, was designed, fabricated, and evaluated. To enhance power reception, two multi-element antenna configurations were designed. End-to-end microwave power transfer experiments were performed with results compared against theoretical calculations and simulations. Consequently, a standard 100 W scalable configuration was designed and simulated to calculate charging time based on MoonBot power requirements over distances upto 1000 m.

The proposed rectenna emphasizes scalability, compact honeycomb structure with increased effective aperture area, and ease of fabrication, making it well-suited for wireless charging of robotic systems. In addition, a simulation methodology was introduced for modelling end-to-end power transfer over distances ranging from a few meters to kilometre-scale.

While this work validates key aspects of the concept, future work will focus on increasing element spacing to reduce mutual coupling, integrating superior diodes for rectifying power levels beyond 1.5 W, enhancing rectifier efficiency across varying load conditions and implementation of multiple rectenna modules in a distributed arrangement with modular deployment capabilities. These contributions will be pivotal towards realizing a practical, scalable microwave-based wireless power receiver systems for lunar robots.

ACKNOWLEDGEMENT

The authors also thank Prof. Naoki Shinohara, Dr. Yang Bo and Mr. Jianwei Jing of Shinohara lab, Kyoto University for their invaluable support in conducting MWPT experiments for the proposed rectenna.

REFERENCES

[1] B. Hussain *et al.*, "Robotics for Space Exploration: From Mars Rovers to Lunar Missions," *Ethical AI Applications*, June 2025.

[2] K. Uno *et al.*, "MoonBot: Modular and On-demand Reconfigurable Robot Towards Moon Base Construction," *IEEE Transactions on Field Robotics*, 2025, Accepted, awaiting publication.

[3] P. Glaser *et al.*, "Illumination Conditions at the Lunar Poles: Implications for Future Exploration," *Planetary and Space Science*, vol. 162, pp. 170–178, 2018.

[4] T. B. Slusser *et al.*, "Surviving Night at the Lunar South Pole: Exploring Viability of Radioisotope Power Systems for a Crewed Rover," in *Thermal & Fluids Analysis Workshop*, USA, 2023.

[5] F. Davies, "Challenges of a Lunar Surface Electrical Power Grid," NASA JSC, Propulsion and Power Division, Tech. Rep., 2023.

[6] R. Bewick, J.-P. Sánchez, and C. R. McInnes, "Use of orbiting reflectors to decrease the technological challenges of surviving the lunar night," in *Proceedings of the International Astronautical Congress (IAC)*, Cape Town, South Africa, 2011.

[7] N. Kawashima, K. Takeda, H. Matsuoka, Y. Fujii, and M. Yamamoto, "Laser energy transmission for a wireless energy supply to robots," in *Proceedings of the International Symposium on Automation and Robotics in Construction (ISARC)*, Ferrara, Italy, 2005.

[8] N. Shinohara, *Wireless Power Transfer via Radiowaves*, 1st ed. Hoboken, NJ, USA: John Wiley & Sons, 2014.

[9] W. C. Brown, "The History of Power Transmission by Radio waves," *IEEE Transactions on Microwave Theory and Techniques*, vol. 32, no. 9, pp. 1230–1242, 1984.

[10] J. Miyasaka *et al.*, "Control for microwave-driven agricultural vehicle – tracking system of parabolic transmitting antenna and vehicle rectenna panel," *Engineering in Agriculture, Environment and Food*, vol. 6, no. 3, pp. 135–140, 2013.

[11] M. Iwashimizu *et al.*, "Study on direction detection in a microwave power transmission system for a Mars observation airplane," in *Wireless Power Transfer Conference (WPTC)*, 2014, pp. 1–4.

[12] Y. Ozawa and N. Tanaka, "Study of electric aircraft charged by beamed microwave power," *IHI Technology & Innovation Review*, vol. 48, no. 2, pp. 29–39, 2015.

[13] M. Furukawa *et al.*, "Wireless power transmission to 10kw output 2.4ghz-band rectenna array for electric trucks application," IEICE Technical Report (in Japanese), Tech. Rep., 2013.

[14] C. Wang *et al.*, "Study and Design of a 2.45-GHz Rectifier Achieving 91% Efficiency at 5-W Input Power," *IEEE Microwave and Wireless Components Letters*, vol. 31, no. 1, pp. 76–79, Jan. 2021.

[15] Dassault Systemes, "CST Microwave Studio," Software, 2024.

[16] Keysight Technologies, "Advanced Design System," Software, 2024.

[17] N. Shinohara and J. Zhou, *Far-Field Wireless Power Transfer and Energy Harvesting*. Norwood, MA, USA: Artech House, 2022.